Crystals of binary rare-earth metal germanides grown in molten indium. Synthesis and structural characterization of Nd_3Ge_5 and Lu_3Ge_4

J. Zhang[1,2], S. Bobev[1]*

[1] Department of Chemistry and Biochemistry, University of Delaware, Newark, Delaware 19716, USA
[2] School of Materials Science and Engineering, Dalian Jiaotong University, Dalian 116028, P.R. China

Reported are the synthesis and the crystal structure determination of a new polymorphic form of the rare-earth metal germanide Nd_3Ge_5. As established by single-crystal X-ray diffraction methods, Nd_3Ge_5 crystallizes in a hexagonal crystal system with the space group $P\bar{6}2c$ (No. 190, $Z = 2$). The unit cell parameters are $a = 6.9964(3)$ Å and $c = 8.5820(8)$ Å. The structure is a derivative of the common structure type AlB_2 (space group $P6/mmm$) where the atoms are stacked in a hexagonal close-packed manner. Digermanide $NdGe_2$ is not known, rather the phase exists as $NdGe_{2-x}$ ($x < 0$) with a sizeable number of germanium vacancies. When the defect concentration reaches $x = 1/3$, the vacant Ge sites can undergo long-range ordering, resulting in the formation of Nd_3Ge_5 (=$NdGe_{1.67}$). Therefore, the atomic arrangement can be described as a 6-fold superstructure of the AlB_2 type structure ($a' = a \times 3^{1/2}$ and $c' = c \times 2$) with flat Ge layers, where every 6th Ge atom is missing; the Ge layers are stacked along the crystallographic c-axis, and are separated by hexagonal layers of rare-earth metal atoms. This is a new polymorph of Nd_3Ge_5, with the other form being orthorhombic and structurally related to another commonly observed structure, that of $ThSi_2$. Besides the structure of Nd_3Ge_5, we also report the structure of the known phase Lu_3Ge_4, which has been previously identified from its powder diffraction pattern but never refined. Lu_3Ge_4 is isotypic with the rest of the $REGe_4$ germanides ($RE = Gd–Tm$) and crystallizes in an orthorhombic crystal system with the space group $Cmcm$ (No. 63, $Z = 4$) with unit-cell parameters $a = 3.9591(8)$ Å; $b = 10.429(2)$ Å; $c = 14.019(3)$ Å.

Keywords: Rare-earth metal germanides; crystal structure; polymorphism; Nd_3Ge_5; Lu_3Ge_4

INTRODUCTION

The crystal structures of the rare-earth metal germanides are diverse [1-3] and still not fully understood. This is even true for the binary phases, where Ge defects abound, and the proper crystallographic characterization has proven to be extremely challenging. Let us take for example the case of the digermanides, many of which were originally thought to be fully stoichiometric $REGe_2$ binary phases (RE = rare-earth element, hereafter) crystallizing with the ubiquitous AlB_2 and α-$ThSi_2$ structure types [3]. However, this rarely holds true, and almost exclusively, non-stoichiometric $REGe_{2-x}$ compounds are formed ($0 \leq x \leq 0.5$) [4-12]. Our own efforts in exploring this rich structural chemistry have been facilitated through the use of the metal flux method [13]. The use of molten In, Sn, Bi or Pb allowed the facile synthesis (at milder conditions) and the crystal growth of several new binary and ternary compounds [4-6,14-20]. Through our previous studies, the reactive nature of the metal flux, and the ability to synthesize new multinary phases from molten metal solutions have come to a full display. This notion can be evidenced from the reports on ternary compounds

such as RE_2InGe_2 (RE = Sm, Gd–Ho, Yb) [14], $RESn_{1+x}Ge_{1-x}$ (RE = Y, Gd–Tm) [16], $REBi_xGe_{2-x}$ (RE = Y, Gd–Tm) [19], and RE_2PbGe_2 [20]. On the other side, owing to its function as a solvent, the metal-flux has played a beneficial role in our attempts to synthesize new compounds/ polymorphs, such as Gd_3Ge_4 [6], RE_3Ge_5 (RE = Sm, Gd, Tb, Dy) [4] or the RE_4Ge_7 (RE = Sm, Gd, Tb, Dy) [18], among others. Employing the flux-growth method, we accessed yet another new polymorph within a well-studied RE–Ge binary system. Herein, we present the synthesis of β-Nd_3Ge_5 (the already known orthorhombic polymorph of Nd_3Ge_5 (Pearson symbol $oF64$) [21] is hereby designated as the α-form). Crystals of β-Nd_3Ge_5 have been grown from the respective elements using In flux, and the structure was elucidated from single-crystal X-ray diffraction methods. β-Nd_3Ge_5 is isotypic with the hexagonal polymorph of Sm_3Ge_5 (Pearson symbol $hP16$) [4]. Additionally, the exploratory work in another RE–Ge binary system led to the discovery of single-crystals of Lu_3Ge_4. While Lu_3Ge_4 has been known as isotypic with the rest of the RE_3Ge_4 germanides for over 30 years [22], its crystal structure had not been fully elucidated prior to this work.

---

* To whom all correspondence should be sent:
E-mail: *bobev@udel.edu*

EXPERIMENTAL

Synthesis

Pure elements—Nd, Lu, Ge and In—all with purity greater than 99.9 % wt metal basis were sourced from Thermo Scientific (formerly Alfa Aesar) and were used as received. Indium was in the form of teardrops, the rest of the elements were chunks. The metals were stored and handled inside an argon-filled glove-box with controlled oxygen and moisture levels below 1 ppm, or under vacuum. Mixtures of the elements in a ratio of *RE*:Ge:In = 3:5:30 were loaded in alumina crucibles (2 cm^3), which were encapsulated in fused silica ampoules. The ampoules were evacuated (*ca.* 10^{-3} Torr) and flame-sealed.

The reaction conditions were identical to those used for the synthesis of Tb$_3$Ge$_5$ and Dy$_3$Ge$_5$ [4]. We used Thermolyne muffle furnace with a microprocessor controller and the following heating/cooling steps: 1) temperature ramp to 1373 K (300 K/h); 2) dwell at 1373 K (3 h); 3) cooling to 773 K (30 K/h). At this point, the reaction mixtures were removed from the furnace and the flux was removed by decanting it, as described in detail previously [14]. Upon opening the sealed tubes, crystals were found and isolated; they were later characterized by single-crystal X-ray diffraction. The bulk of the products was confirmed by powder X-ray diffraction. In both experiments, there were crystals from multiple phases present. In the case of the Nd-Ge reaction, besides the new hexagonal polymorph of Nd$_3$Ge$_5$, we also encountered crystals from Nd$_4$Ge$_7$ [18]. In the case of the Lu-Ge reaction, there was a monoclinic phase that is still not fully characterized (presumed to be a variant of LuGe$_{2-x}$), as well as crystals of Lu$_3$Ge$_4$, which to date had only been studied in polycrystalline form [22]. The crystals were sub-millimeter in size and did not have well-defined morphologies; they exhibited a silver-metallic luster and were found to be air- and moisture-stable over extended periods of time (greater than 12 months).

This study also confirmed what had been noted in prior publications [4, 23], namely, that the cooling rate is of particular importance with regard to the formation of either *RE*$_3$Ge$_5$ polymorph. Specifically, slower cooling rates (*ca.* 5 K/h) favor the orthorhombic α-form of the Nd$_3$Ge$_5$ phase, while faster cooling (*ca.* 30 K/h) affords the hexagonal β-Nd$_3$Ge$_5$ polymorph. Attempts to make polycrystalline samples of β-Nd$_3$Ge$_5$ through direct fusion of the corresponding elements (arc-melting) were not successful. These observations are

104

suggestive of the β-polymorph being metastable at ambient pressure and temperature.

Powder and single-crystal X-ray diffraction

X-ray powder diffraction patterns were taken at room temperature on a Rigaku Miniflex powder diffractometer using filtered Cu Kα radiation. The scans were in *θ-θ* mode ($2\theta_{max} = 80°$) with a typical step-size of 0.05° and 3 sec/step (or 5 sec/step) counting time. The collected powder patterns were used for phase identification only, which was done using JADE v.6.5. The presence of multiple phases, combined with the low resolution of the instrument (and the lack of monochromated radiation) precluded the detailed analysis of the powder diffraction patterns; we only note that intensities and the positions of the strong peaks (experimental and the calculated from the crystal structures) were in excellent agreement. The weak peaks that are the telltale sign of the long-range defect ordering in β-Nd$_3$Ge$_5$ (Figure 1) could only be observed by single-crystal X-ray diffraction (*vide infra*).
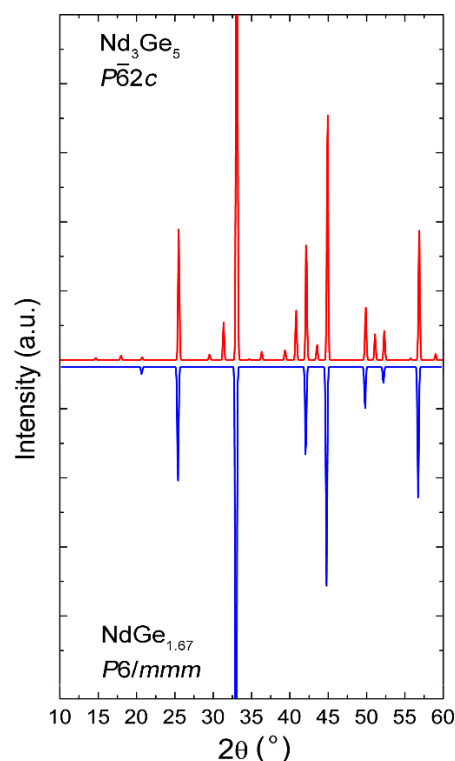

Figure 1. Simulated powder X-ray diffraction patterns for two closely related structural models: i) stoichiometric Nd$_3$Ge$_5$ (red trace, space group $P\bar{6}2c$), and ii) non-stoichiometric NdGe$_{2-x}$ ($x \sim 0.3$) with the AlB$_2$-type structure (blue trace, space group $P6/mmm$). The reflections at low angle that arise from the ordering of the Ge defects in NdGe$_{2-x}$ and increase the periodicity are expected to be less than 1-2% of the intensity of the strongest peak, thus, difficult to measure experimentally.

X-ray single-crystal diffraction data collections were carried out on a Bruker CCD-based diffractometer using monochromated Mo Kα radiation. The crystals were mounted on glass fibers using oil, which hardens and immobilizes the crystal at the tip of the fiber at the data collection temperature of 120 K (maintained by a cold nitrogen gas stream). Intensity data for crystals from both compounds were collected in batch runs at different ω and φ angles, covering reciprocal space with redundancy of at least a factor of five. This was necessary for the semi-empirical absorption corrections, based on equivalent reflections, which were applied with the program SADABS [24]. The Bruker-supplied software was used for management of the data collection (SMART) [25] and integration of the 2D-frames, and for unit cell parameter refinement, taking into account all reflections (SAINT) [26]. The

structures were refined on F^2 using the SHELX package [27]; the coordinates from the isostructural Sm_3Ge_5 [4] were used as the starting model for β-Nd_3Ge_5; the coordinates from the isostructural Tm_3Ge_4 [6] were used as the starting model for refining the structure of Lu_3Ge_4. All atomic positions were refined with anisotropic displacement parameters, leading to quick convergences and excellent goodness of fit. Final residuals and other relevant data collection and structure refinement parameters are summarized in Table 1. Positional and equivalent displacement parameters are given in Table 2.

The crystallographic information files (CIF) have also been deposited CIF files with additional information are deposited in the Cambridge Crystallographic Data Centre (CCDC) with deposition numbers 2365206 (β-Nd_3Ge_5) and 2365207 (Lu_3Ge_4).

Table 1. Selected single crystal collection and refinement parameters for β-Nd_3Ge_5 and Lu_3Ge_4.

Empirical formula	Nd_3Ge_5	Lu_3Ge_4
Formula weight	795.67	815.27
Space group, Z	$P\overline{4}2c$, 2	$Cmcm$, 4
Radiation, λ		Mo Kα, 0.71073 Å
Temperature		120(2) K
Unit cell parameters		
a (Å)	6.9964(3)	3.9591(8)
b (Å)	6.9964(3)	10.429(2)
c (Å)	8.5820(8)	14.019(3)
V (Å^3)	363.80(4)	578.85(19)
Crystal size (mm)	0.05×0.05×0.03	0.08×0.05×0.04
ρ_{calc} (g/cm^3)	7.26	9.36
μ (cm^{-1})	412.3	709.8
Data:parameters	327:17	454:28
Absorption correction method	Semi-empirical, based on equivalents	
Final R1^a and wR2^b [$I>2\sigma_I$]	R1 = 0.0193 wR2 = 0.0437	R1 = 0.0272 wR2 = 0.0494
Final R1^a and wR2^b [all data]	R1 = 0.0253 wR2 = 0.0463	R1 = 0.0366 wR2 = 0.0513
Largest peak/hole	0.73/–1.56 e$^-$/Å^3	1.96/–2.74 e$^-$/Å^3

^{a} R1 = $\sum||F_o| - |F_c||/\sum|F_o|$
^{b} wR2 = $[\sum[w(F_o^2 - F_c^2)^2]/\sum[w(F_o^2)^2]]^{1/2}$, where w = $1/[\sigma^2F_o^2 + (A \cdot P)^2 + B \cdot P]$,
P = $(F_o^2 + 2F_c^2)/3$; A and B are the respective weight coefficients

Table 2. Atomic coordinates and equivalent displacement parameters (U_{eq}[a]) for β-Nd_3Ge_5 and Lu_3Ge_4.

Atom	Site	x/a	y/b	z/c	U_{eq} (Å^2)
			Nd_3Ge_5		
Nd1	6g	0.3318(1)	0	0	0.0067(1)
Ge1	6h	0.3887(2)	0.3309(2)	1/4	0.0096(2)
Ge2	2d	1/3	2/3	1/4	0.0079(4)
Ge3	2b	0	0	1/4	0.0086(4)
			Lu_3Ge_4		
Lu1	8f	0	0.3227(1)	0.0971(1)	0.0083(2)
Lu2	4c	0	0.0502(1)	1/4	0.0082(2)
Ge1 [b]	8f	0	0.010(2)	0.010(1)	0.008(2)
Ge2	8f	0	0.6224(1)	0.1084(1)	0.0093(3)
Ge3	4c	0	0.7806(2)	1/4	0.0085(4)

[a] U_{eq} is defined as 1/3 of the trace of the orthogonalized U_{ij} tensor.
[b] Ge1 should be at the origin (site 4a), however, its anisotropic displacement parameter is suggestive of the atom being displaced; there Ge1 is offset to a site 8f with fixed 50% occupancy.

RESULTS AND DISCUSSION

Crystal structure of Nd_3Ge_5

A schematic representation of the structure of the new hexagonal polymorphs of Nd_3Ge_5 is shown in Figure 2.
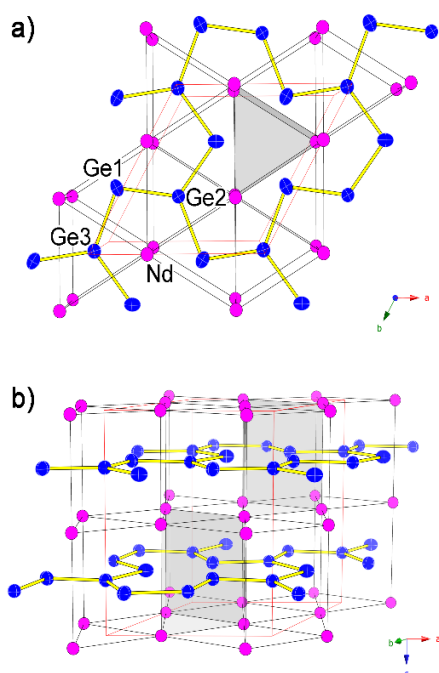

Figure 2. Crystal structure of the hexagonal β-Nd_3Ge_5, shown in two different orientations with the unit cell outlined. Symmetry independent sites are labeled. The drawings are with anisotropic displacement parameters at the 95% probability level. The rare-earth metal atoms are shown in magenta and the Ge atoms are depicted in blue. Ge–Ge bonds are shown as yellow cylinders, while the Nd–Nd contacts are represented with thin black lines, illustrating the trigonal prisms formed by the rare-earth metal atoms and the way they are fused together. The trigonal prisms shaded in light grey do not host Ge atoms.

Only a brief account of the structure will be given here; for a more comprehensive description we refer the reader to the report on the isostructural RE_3Ge_5 compounds [4, 23]. Using the already communicated ideas, the structure can be understood as a variant of the non-stoichiometric $NdGe_{2-x}$ phase (AlB_2 structure type) when $x = 1/3$. For this to happen, ordering of the vacant Ge sites (every 6th atom from the honeycomb-like arrangement) must occur in a periodic manner, which leads to the atomic arrangement shown in Figure 2. Therefore, the unit cell of the sub-structure and the super-structure will be related via the simple geometric relationship $a' \approx a \times 3^{1/2}$. In addition, since the newly formed layers are not stacked in the same sequence as in the AlB_2-structure, but are staggered, the c-edge of the unit cell must be doubled ($c' \approx c \times 2$), yielding an overall 6-fold increase of the cell volume. The structure can also be envisioned as built from triangular prisms made of rare-earth metal atoms that share common faces, and which are centered by germanium atoms (Figure 2). Of worthwhile mention is the fact that not all of these prisms are filled, in fact, one out of every six is empty.

As discussed in earlier publications [4, 23], even if one were to ignore the relatively weak superstructure reflections, there are several indicators from the structure refinement, which would suggest that the AlB_2-type model cannot be fitted with the desired accuracy. Since there is just one crystallographic site for the Ge atoms in the AlB_2-type structure (space group $P6/mmm$), on a special position with Wyckoff symbol 2d, the Ge–Ge distances will only be interrelated by the lattice

parameters. This amounts to unrealistically short Ge–Ge contacts (on the order of 2.2 Å), much shorter than the expected single-bonded Ge–Ge distance of 2.44 Å in elemental Ge [28]. The 2.2 Å separation between Ge atoms is even shorter than the possible Ge=Ge distance, that is if the atoms were sp^2-hybridized like the carbon atoms in graphite. Additionally, the electron density on that site is rather "smeared" and the anisotropic displacement parameter for Ge is grossly elongated in the *ab*-plane. All of the above are serious delinquencies of the description of non-stoichiometric NdGe$_{2-x}$ as a phase with the AlB$_2$-type structure.

In the 6-fold superstructure (Figure 3), due to the regularity of the vacancies, the Ge layers undergo a small reconstruction (Figure 3), and the Ge–Ge distances become normal—they now measure from 2.542(1) Å to 2.565(1) Å (Table 3), along with the Ge–Ge–Ge bonds angles decreasing from 120º to *ca.* 104.5º. Such metrics are comparable to the ones in many other binary germanides such as RE_3Ge$_5$ (RE = Sm, Gd, Tb, Dy) [4,23], RE_3Ge$_4$ (RE = Gd through Tm) [6], RE_4Ge$_7$ (RE = La–Nd, Sm) [18]. Ultimately, the Nd–Ge contacts (due to the defects, the rare-earth metal is surrounded by 10 next nearest germanium neighbors) are comparable to those found in the latter compounds and measure between *ca.* 3.03 Å and *ca.* 3.47 Å. A comparison of the RE–Ge distances for the known RE_3Ge$_5$ compounds with this structure shows a good correlation with the decreasing size of the rare-earth metal cations when moving across the lanthanide series. The Ge–Ge distances, however, are invariant upon changing the RE metal.
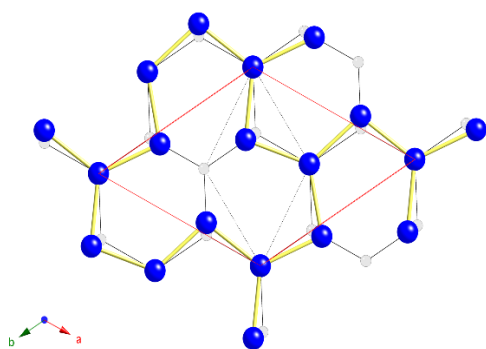

Figure 3. Schematic representation of the distortion of the honeycomb Ge-layers (idealized NdGe$_2$ in the hexagonal AlB$_2$ type structure, grey spheres) and the actual topology of the Ge net in hexagonal β-Nd$_3$Ge$_5$. The corresponding subcell-supercell interrelation is also illustrated by dotted black and solid red lines, respectively.

Table 3. Selected interatomic distances (Å) in β-Nd$_3$Ge$_5$ and Lu$_3$Ge$_4$.

Atom pair		Distance
	β-Nd$_3$Ge$_5$	
Ge1–	Ge3	2.542(1)
	Ge2	2.565(1)
	Nd × 2	3.0331(8)
	Nd × 2	3.0631(8)
	Nd × 2	3.466(1)
Ge2–	Ge1 × 3	2.565(1)
	Nd × 6	3.1730(2)
Ge3–	Ge1 × 3	2.542(1)
	Nd × 6	3.1608(4)
Nd–	Ge1 × 2	3.0331(8)
	Ge1 × 2	3.0631(8)
	Ge3 × 2	3.1608(4)
	Ge2 × 2	3.1730(2)
	Ge1 × 2	3.466(1)
	Lu$_3$Ge$_4$	
Ge1–	Ge2 × 2 [a]	2.683(9)
	Ge2 × 2	2.929(9)
	Lu1 × 2	2.97(2)
	Lu1 × 2	2.97(2)
	Lu2 × 2	3.39(2)
Ge2–	Ge3	2.581(2)
	Ge1 × 2	2.683(9)
	Lu2 × 2	2.902(1)
	Lu1	2.918(2)
	Lu1 × 2	2.959(1)
	Lu1	3.025(2)
Ge3–	Ge2 × 2	2.581(2)
	Lu2	2.813(2)
	Lu1 × 4	2.9685(7)
	Lu2 × 2	3.113(2)

[a] In the event Ge1 is refined at the origin (0,0,0), the distance Ge1–Ge2 is 2.803(1) Å (×4).

The last comment we would like to make in this sub-section concerns the well-known fact the rare-earth metal germanides with around 50-67 %at. Ge show large stoichiometry breadths, i.e., their chemical formulae are REGe$_{2-x}$ ($0 \leq x \leq 0.5$). For the early rare-earth metals, the prevailing structure type of the basic structure is the tetragonal α-ThSi$_2$ (Pearson symbol *tI*12). Thus, it is not surprising that the α-ThSi$_2$ derivatives, the orthorhombic α-form of the Nd$_3$Ge$_5$ phase (space group *Fdd*2, 6-fold superstructure of NdGe$_{2-x}$ with x = 1/3), and the Nd$_4$Ge$_7$ phase (space group *C*222$_1$, 4-fold superstructure of NdGe$_{2-x}$ with x = 1/4), are already known. It is surprising, however, that a variant of the layered hexagonal AlB$_2$ type structure (Pearson symbol *hP*3), which is a lot more common for the mid-to-late rare-earth metals is found for the β-form of the Nd$_3$Ge$_5$ phase. This dimorphism is not indicated in the corresponding phase diagram [29],

which only suggests α-NdGe$_{2-x}$ (low temperature form, space group *Imma*) and β-NdGe$_{2-x}$ (high temperature form, space group *I*4$_1$/*amd*) to exist between 60-61.6 %at. Our own work has not shown that tetragonal to orthorhombic (*I*4$_1$/*amd* to *Imma*) distortion can be observed as a function of the cooling rates. Since the phase NdGe$_{2-x}$ is indicated as congruently melting, it is entirely possible that the high temperature polymorph can be retained at room temperature. However, the experiments and the hexagonal structure described here, obtained from crystals grown via the flux growth technique, are suggestive of the hexagonal form to be metastable (kinetic) phase. Since the molten flux alters the nucleation and growth conditions, β-Nd$_3$Ge$_5$ can only be "trapped" when using flux growth and fast cooling rates.

Crystal structure of Lu$_3$Ge$_4$

The "average" structure of Lu$_3$Ge$_4$ belongs to the W$_3$CoB$_3$ type (centrosymmetric space group *Cmcm*, Pearson symbol *oS*28). We use the term "average" because there are some subtleties to it, which Oleksun and Bodak did not capture 30 years ago [22], when they assigned the structure of *RE*$_3$Ge$_4$ (*RE* = Er, Ho, Tm, Lu) and provided structure refinement for Er$_3$Ge$_4$, based on powder X-ray diffraction data. In the 1994 paper, the structures of the remaining members of the family were not refined, only their unit cell parameters were determined [22].

In our previous work on Gd$_3$Ge$_4$ [6], we noted the abnormal anisotropic displacement parameter of Ge1 (at 0, 0, 0). Since refinements of the site occupation factor ruled out Ge defects as a root-cause for this anomaly, positional disorder was introduced—this atomic position was shifted off of the origin (at 0, *y*, *z*) and was refined as a split site, occupied statistically. This led to a normal thermal parameter and a flat difference Fourier map.

The same problems with the structure refinements were encountered for Lu$_3$Ge$_4$ as well. During the first refinement cycles, the structure was refined using the coordinates already reported for the Er$_3$Ge$_4$ structure [22]. The refinement cycles with isotropic displacement parameters confirmed the model, but the refinement converged to higher than normal R-values. Refinements with anisotropic displacement parameters improved the residuals, but turned up the unusual elongation on Ge1 (Wyckoff site 4*c*). The structure was then refined by freeing the occupation factor of this site, which showed no deviations greater than 3σ (similar to freeing the site occupation factors on all other atoms, which had well-behaved anisotropic

displacement parameters). Therefore, the Ge1 was split (Figure 4b) to two 50% occupied sites. As shown in Figure 3, a model that avoids placing Ge in nearly square-planar coordination of other Ge atoms is clearly preferred. Offsetting Ge1 allows all Ge–Ge distances to be in the more typical range from 2.58 Å to 2.68 Å (Table 3), along with some the Ge–Ge–Ge angles increasing from *ca.* 90º to *ca.* 95º. Had Ge1 been treated as occupying the special position at the origin, the Ge–Ge distances would have been longer than 2.8 Å.

Overall, the structure can be viewed as an intergrowth of CrB and AlB$_2$-like fragments. This addition of motifs creates a Ge layered-network, with the slabs being separated by Lu atoms. The typical for rare-earth atoms arrangements of fused trigonal prisms are on display in Figure 4.
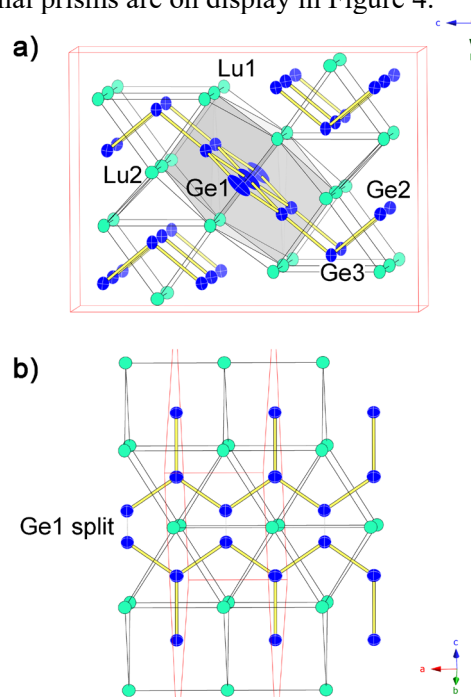

Figure 4. (a) Crystal structure of the Lu$_3$Ge$_4$, shown in with anisotropic displacement parameters at the 95% probability level. Symmetry independent sites are labeled and the unit cell is outlined. The Lu atoms are shown in light green and the Ge atoms are depicted in blue. Ge–Ge bonds are shown as yellow cylinders, while the Lu–Lu contacts are represented with thin black lines, illustrating the trigonal prisms formed by the rare-earth metal atoms and the way they are fused together. The trigonal prisms shaded in light grey do not host Ge atoms. The peculiar elongation of the anisotropic displacement parameter of Ge1 (at 0, 0, 0) suggests that the atom would prefer to be "inside" the trigonal prism, not in the center of its rectangular face. (b) Crystal structure of the Lu$_3$Ge$_4$, shown again in with anisotropic displacement parameters at the 95% probability level and in a different projection. Ge1 atom has been offset from the special position and is now 50% occupied.

For further structural discussion, the reader is referred to a preceding publication addressing the structure revision for all known RE_3Ge_4 phases, excluding Lu_3Ge_4 [6], for which the full structure elucidation is reported in this article.

CONCLUSIONS

Crystals of hexagonal β-Nd_3Ge_5 phase, a previously unknown polymorph of Nd_3Ge_5 were obtained using In flux, and the structure was elucidated from single-crystal X-ray diffraction methods. Considering that the structure is ordered, has triangular Nd lattice and no center of symmetry, one may expect competing magnetic interactions that warrant further investigations. The application of the same synthetic method also affords single-crystals of Lu_3Ge_4, a material that has been known for over 30 years [22], but not available in single-crystalline form. Given that several other Lu-Ge binaries are superconductors, including $LuGe_2$ [30,31], and $LuGe_3$ [32], it can be suggested that Lu_3Ge_4 should also be evaluated as a superconductor.

REFERENCES

1. A. Szytula, J. Leciejewicz (eds.), Handbook of crystal structures and magnetic properties of rare earth intermetallics, CRC Press, Boca Raton, FL, 1994.
2. A. Iandelli, A. Palenzona, Crystal chemistry of intermetallic compounds, in: Handbook on the physics and chemistry of rare earths, K. A. Gschneidner Jr, L. Eyring (eds.) vol. 2, North Holland, Amsterdam, 1979, p. 1.
3. P. Villars, L. D. Calvert, Pearson's Handbook of crystallographic data for intermetallic phases, second edn., American Society for Metals, Materials Park, OH, 1991.
4. P. H. Tobash, D. Lins, S. Bobev, N. Hur, J.D. Thompson, J. L. Sarrao, *Inorg. Chem.,* **45**, 7286 (2006).
5. S.-P. Guo, J. J. Meyers, P. H. Tobash, S. Bobev, *J. Solid State Chem.,* **192**, 16 (2012).
6. P. H. Tobash, G. DiFilippo, S. Bobev, N. Hur, J. D. Thompson, J. L. Sarrao, *Inorg. Chem.*, **46**, 8690 (2007).
7. G. Venturini, I. Ijjaali, B. Malaman, *J. Alloys Compds.*, **289**, 168 (1999).
8. A. M. Guloy, J. D. Corbett, *Inorg. Chem.*, **30**, 4789 (1991).
9. G. Venturini, I. Ijjaali, B. Malaman *J. Alloys Compds.*, **284**, 262 (1999).
10. G. Venturini, I. Ijjaali, B. Malaman *J. Alloys Compds.*, **285**, 194 (1999).
11. G. Venturini, I. Ijjaali, B. Malaman, *J. Alloys Compds.*, **289**, 116 (1999).
12. O. Zaharko, P. Schobinger-Papamantellos, C. Ritter, *J. Alloys Comp.*, **280**, 4 (1998).
13. M. G. Kanatzidis, R. Pöttgen, W. Jeitschko, *Angew. Chem., Int. Edn.*, **44**, 6996 (2005).
14. P. H. Tobash, D. Lins, S. Bobev, A. Lima, M. F. Hundley, J. D. Thompson, J. D. Sarrao, *Chem. Mater.*, **17**, 5567 (2005).
15. P. H. Tobash, S. Bobev, *J. Am. Chem. Soc.*, **128**, 3532 (2006).
16. P. H. Tobash, J. J. Meyers, G. DiFilippo, S. Bobev, F. Ronning, J. D. Thompson, J. L. Sarrao, *Chem. Mater.*, **20**, 2151 (2008).
17. S. Bobev, E. D. Bauer, J. D. Thompson, J. L. Sarrao, G. J. Miller, B. Eck, R. Dronskowski, *J. Solid State Chem.*, **177**, 3545 (2004).
18. J. Zhang, P. H. Tobash, W. D. Pryz, D. J. Buttey, N. Hur, J. D. Thompson, J. L. Sarrao, S. Bobev, *Inorg. Chem.*, **52**, 953 (2013).
19. J. Zhang, B. Hmiel, A. Antonelli, P. H. Tobash, S. Bobev, S. Saha, K. Kirshenbaum, R. L. Greene, J. Paglione, *J. Solid State Chem.*, **196**, 586 (2012).
20. N.T. Suen, J. Hooper, E. Zurek, S. Bobev, *J. Am. Chem. Soc.*, **134**, 12708 (2012).
21. P. Schobinger-Papamantellos, K. H. L. Buschow, *J. Magn. Magn. Mater.*, **82**, 99 (1989).
22. O. Ya. Oleksyn, O. I. Bodak, *J. Alloys Compds.*, **210**, 19 (1994).
23. P. H. Tobash, S. Bobev, F. Ronning, J. D. Thompson, J. L. Sarrao, *J. Alloys Compds.,* **488**, 533 (2009).
24. SADABS NT, version 2.10, Bruker Analytical X-Ray Systems, Inc., Madison, WI, 2001.
25. *SMART NT*, Version 5.63, Bruker Analytical X-ray Systems Inc., Madison, WI, USA, 2003.
26. *SAINT NT*, Version 6.45, Bruker Analytical X-ray Systems Inc., Madison, WI, USA, 2003.
27. G. M. Sheldrick, *Acta Crystallogr. C*, **71**, 3 (2015).
28. L. Pauling, The nature of the chemical bond, third edn., Cornell University Press, Ithaca, NY, 1960.
29. T. B. Massalski, Binary alloy phases diagrams, American Society for Metals, Materials Park, OH, 1990.
30. J. Zhang, F. Ding, J.-J. Lee, G. Shan, S. Bobev, *Inorg. Chem.*, **59**, 16853 (2020).
31. Y. R. Chung, H. H. Sung, W. H. Lee, *Phys. Rev. B: Condens. Matter Mater. Phys.*, **70**, 052511 (2004).
32. J.-M. Hübner, M. Bobnar, L. Akselrud, Y. Prots, Y. Grin, U. Schwarz, *Inorg. Chem.*, **57**, 10295 (2018).